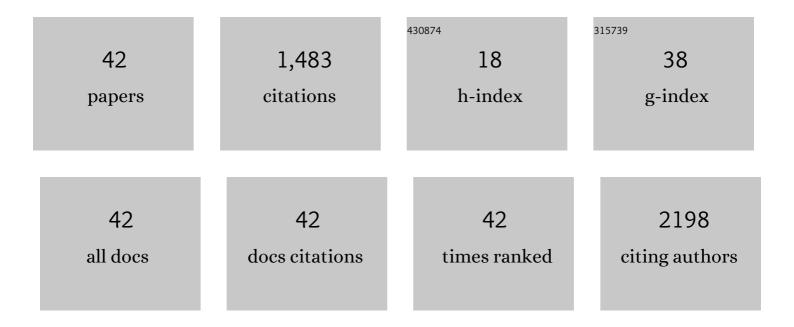
## Hong Huang

List of Publications by Year in descending order

Source: https://exaly.com/author-pdf/8949782/publications.pdf

Version: 2024-02-01



#	Article	IF	CITATIONS
1	Construction of Heterostructured g-C <sub>3</sub> N <sub>4</sub> /Ag/TiO <sub>2</sub> Microspheres with Enhanced Photocatalysis Performance under Visible-Light Irradiation. ACS Applied Materials & Interfaces, 2014, 6, 14405-14414.	8.0	595
2	Synthesis of ternary g-C3N4/Ag/γ-FeOOH photocatalyst: An integrated heterogeneous Fenton-like system for effectively degradation of azo dye methyl orange under visible light. Applied Surface Science, 2017, 425, 862-872.	6.1	87
3	Synthesis of core-shell ZnO/oxygen doped g-C3N4 visible light driven photocatalyst via hydrothermal method. Journal of Alloys and Compounds, 2017, 708, 853-861.	5.5	72
4	Synthesis of porous ZnO/TiO2 thin films with superhydrophilicity and photocatalytic activity via a template-free sol–gel method. Surface and Coatings Technology, 2014, 258, 531-538.	4.8	67
5	Effect of polyethylene glycol on hydrophilic TiO2 films: Porosity-driven superhydrophilicity. Surface and Coatings Technology, 2010, 204, 3954-3961.	4.8	57
6	Superhydrophilicity of TiO2/SiO2 thin films: Synergistic effect of SiO2 and phase-separation-induced porous structure. Surface and Coatings Technology, 2012, 213, 126-132.	4.8	55
7	Synergistic effect of homogeneously dispersed PANI-TiN nanocomposites towards long-term anticorrosive performance of epoxy coatings. Progress in Organic Coatings, 2019, 130, 158-167.	3.9	52
8	The diacetone acrylamide crosslinking reaction and its control of coreâ€shell polyacrylate latices at ambient temperature. Journal of Applied Polymer Science, 2012, 123, 1822-1832.	2.6	43
9	Preparation of PE-EPDM based phase change materials with great mechanical property, thermal conductivity and photo-thermal performance. Solar Energy Materials and Solar Cells, 2019, 200, 109988.	6.2	38
10	pH-driven phase separation: Simple routes for fabricating porous TiO2 film with superhydrophilic and anti-fog properties. Ceramics International, 2015, 41, 7573-7581.	4.8	31
11	Preparation of nanosheet-based spherical Ti/SnO2-Sb electrode by in-situ hydrothermal method and its performance in the degradation of methylene blue. Electrochimica Acta, 2021, 398, 139335.	5.2	31
12	Multimorphologies nano-ZnO preparing through a simple solvothermal method for photocatalytic application. Materials Letters, 2015, 141, 294-297.	2.6	24
13	Birnessite manganese oxide nanosheets assembled on Ni foam as high-performance pseudocapacitor electrodes: Electrochemical oxidation driven porous honeycomb architecture formation. Applied Surface Science, 2018, 458, 10-17.	6.1	23
14	In-situ growth of lepidocrocite on Bi2O3 rod: A perfect cycle coupling photocatalysis and heterogeneous fenton-like process by potential-level matching with advanced oxidation. Chemosphere, 2018, 210, 334-340.	8.2	22
15	Superhydrophilic porous TiO2 film prepared by phase separation through two stabilizers. Applied Surface Science, 2011, 257, 4774-4780.	6.1	19
16	Construction of Ti3+-TiO2-C3N4por compound coupling photocatalysis and Fenton-like process: Self-driven Fenton-like process without extra H2O2 addition. Chemosphere, 2020, 241, 125022.	8.2	19
17	Construction of TiO2-Fe-C3N4 compound: Promotion of interfacial charge transfer effect through facile energy level alignment. Journal of Alloys and Compounds, 2019, 781, 140-148.	5.5	18
18	Formateâ€Selective CO <sub>2</sub> Electrochemical Reduction with a Hydrogenâ€Reductionâ€Suppressing Bronze Alloy Hollowâ€Fiber Electrode. ChemSusChem, 2020, 13, 6594-6601.	6.8	18

Hong Huang

#	Article	IF	CITATIONS
19	Strong effect of multi-electron oxygen reduction reaction on photocatalysis through the promotion of interfacial charge transfer. Applied Catalysis B: Environmental, 2019, 252, 41-46.	20.2	17
20	High-performance adjustable manganese oxides hybrid nanostructure for supercapacitors. Electrochimica Acta, 2021, 381, 138213.	5.2	17
21	Facile synthesis of the Ti3+–TiO2–rGO compound with controllable visible light photocatalytic performance: GO regulating lattice defects. Journal of Materials Science, 2018, 53, 12770-12780.	3.7	16
22	Polyaniline encapsulated α-zirconium phosphate nanosheet for enforcing anticorrosion performance of epoxy coating. Journal of Coatings Technology Research, 2021, 18, 999-1012.	2.5	16
23	Synthesis and structure investigation of hexamethylene diisocyanate (HDI)-based polyisocyanates. Research on Chemical Intermediates, 2017, 43, 2799-2816.	2.7	15
24	Tuning Mn2+ additive in the aqueous electrolyte for enhanced cycling stability of birnessite electrodes. Electrochimica Acta, 2019, 298, 678-684.	5.2	14
25	Ethylene-Propylene Terpolymer-Modified Polyethylene-Based Phase Change Material with Enhanced Mechanical and Thermal Properties for Building Application. Industrial & Engineering Chemistry Research, 2019, 58, 179-186.	3.7	14
26	The effect of electrolyte cation on electrochemically induced activation and capacitive performance of Mn3O4 electrodes. Electrochimica Acta, 2019, 324, 134894.	5.2	13
27	Redispersibility of Acrylate Polymer Powder and Stability of Its Reconstituted Latex. Journal of Dispersion Science and Technology, 2011, 32, 1279-1284.	2.4	9
28	Polymerization-induced phase separation in the preparation of macroporous TiO2/SiO2 thin films. Ceramics International, 2014, 40, 919-927.	4.8	9
29	Study on bifunctional acyldiphenylphosphine oxides photoinitiator for free radical polymerization. European Polymer Journal, 2022, 168, 111093.	5.4	9
30	Morphology-controlled synthesis of Ti-doped α-Fe2O3 nanorod arrays as an efficient photoanode for photoelectrochemical applications. Research on Chemical Intermediates, 2018, 44, 2365-2378.	2.7	8
31	A new carbazolylâ€basedacylphosphine oxide photoinitiator with high performance and low migration. Journal of Polymer Science, 2022, 60, 52-61.	3.8	8
32	Synthesis of acrylate microemulsion modified by alkoxy silane. Journal Wuhan University of Technology, Materials Science Edition, 2008, 23, 212-217.	1.0	6
33	A recycling model of excess toluene diisocyanate isomers in the preparation of polyurethane prepolymer. Journal of Applied Polymer Science, 2013, 127, 2176-2183.	2.6	6
34	Enhancing Thermal Conductivity and Photo-Driven Thermal Energy Charging/Discharging Rate of Annealed CMK-3 Based Phase Change Material. Nanomaterials, 2019, 9, 364.	4.1	6
35	Large-molecular-weight acyldiphenylphosphine oxides as low-mobility type I photoinitiator for radical polymerization. European Polymer Journal, 2022, 175, 111380.	5.4	6
36	Influence of carboxyl groups on the particle size and rheological properties of polyacrylate latices. Journal Wuhan University of Technology, Materials Science Edition, 2010, 25, 492-498.	1.0	5

Hong Huang

#	Article	IF	CITATIONS
37	Pyrolysis study of waterborne polyurethane. Journal Wuhan University of Technology, Materials Science Edition, 2010, 25, 479-483.	1.0	4
38	Preparation and Formation Mechanism of Superhydrophilic Porous TiO2 Films Using Complexing Agents as Pore-Forming Materials. Science of Advanced Materials, 2014, 6, 9-17.	0.7	4
39	Electrostatic self-assembled PTh/Ag/protonated g-C3N4 nanocomposite with remarkable photocatalytic degradation for organic pollutants. Colloids and Surfaces A: Physicochemical and Engineering Aspects, 2022, 649, 129438.	4.7	4
40	Construction of Three-Dimensional Network Structure in Polyethylene-EPDM-Based Phase Change Materials by Carbon Nanotube with Enhanced Thermal Conductivity, Mechanical Property and Photo-Thermal Conversion Performance. Polymers, 2022, 14, 2285.	4.5	3
41	Accelerated Fe(III)/Fe(II) cycle couples with in-situ generated H2O2 boosting visible light-induced Fenton-like oxidation. Separation and Purification Technology, 2022, 299, 121688.	7.9	2
42	Controllable electrochemical activation of Mn3O4: Anion effect on phase transition, morphology and capacitive performance. Electrochimica Acta, 2022, 416, 140281.	5.2	1